XLI CILAMCE
XLI Ibero-Latin American Congress on Computational Methods in Engineering
16-19 November, 2020 FOZ DO IGUAÇU PARANÁ - BRAZIL

# Comparison of Generalized/eXtended Finite Element Methods for Quasi-Brittle Media Cracking Problems

Larissa Novelli[1], Humberto A. da S. Monteiro[1], Thaianne S. de Oliveira[1], Gabriela M. Fonseca[1], Roque Luiz da S. Pitangueira[1], Felício B. Barros[1]

[1]*Dept. of Structural Engineering, Federal University of Minas Gerais*
*Pres. Antônio Carlos, 6627, School of Engeneering - Bulding 1, Pampulha, Belo Horizonte/MG, Brazil*
*larissan@ufmg.br, hmonteiro@ufmg.br, thaiannesimo@gmail.com, gmarinhofonseca@gmail.com, roque@dees.ufmg.br, felicio@dees.ufmg.br*

**Abstract.** This work presents a comparative study of the application of the Generalized/eXtended Finite Element Method (GFEM) in the solution of cracking problems. Different strategies are performed: Polynomial enrichment strategy with the GFEM and numerical enrichment strategy with and without Stable Generalized Finite Element Method (SGFEM) procedure. The numerical enrichment strategy is based on global-local analysis. For this strategy, the nonlinear analysis is performed in the global problem and a local problem is solved in the end of each converged step. The local solution is used as numerical enrichment for next incremental step of the global problem. This local problem, solved with a fine mesh, is a subdomain of the global problem in the cracking region of the problem. For the application of the polynomial enrichment strategy, the same subdomain of global problem is enriched with prescribed polynomial functions. The smeared cracking model is used as elastic-degradation constitutive model to simulate the behavior of quasi-brittle media. The implementations have been performed in the INSANE (*Interactive Structural Analysis Environment*) system, a free software developed at Department of Structural Engineering of Federal University of Minas Gerais. Numerical example of a two-dimensional problem (2D) is presented for validation and comparison of the strategies. Besides, the results are compared with experimental data and reference solutions obtained via classical Finite Element Method (FEM).

**Keywords:** Global-local, Polynomial enrichment, Stable generalized FEM, Generalized FEM, Nonlinear Analysis

## 1 Introduction

The Generalized/eXtended Finite Element Method (GFEM) [1, 2] emerged from the difficulties of the FEM to solve cracking problems due to the need for a high degree of mesh refinement. This method consist in enriching of the standard FEM approximation. The partition of unity functions (PoU) are enriched with functions that represent *a priori* knowledge of the problem solution. This enriched functions can be of different types, such as polynomial functions, Heaviside functions or numerically built functions.

Despite of the advantages of the use of GFEM, this method can lead to ill-conditioning of the stiffness matrix. The Stable GFEM (SGFEM) was proposed by Babuška and Banerjee [3] to deal with this shortcoming. In this method, the GFEM is modified by subtracting from the enrichment function its FE interpolant. Posteriorly, this method presented also a good performance for the blending elements issues.

In this paper is presented a comparison between different enrichment strategies of GFEM and SGFEM in physically nonlinear analysis. The polynomial functions and numerically built functions are used as enrichment functions. The numerical functions are obtained from global-local strategy. This strategy, named $\text{GFEM}^{\text{GL}}$, was proposed by Duarte and Kim [4] and is applied in simulations in two-scales.

The implementation was performed in the INSANE (INteractive Structural aNalysis Enviroment) system [5]. This software presents resources for physically nonlinear analysis, the GFEM and SGFEM techniques and an unificate framework for constitutive models.

## 2 Generalized/eXtended Finite Element Methods

In the GFEM method, the shape functions are obtained by the product of the PU and the enrichment functions that are denominated local approximate functions. The shape function $\phi_{ji}(x)$ for a node $x_j$ is given by eq. (1).

$$\{\phi_{ji}\}_{i=1}^{q_j} = N_j(x)\{L_{ji}(x)\}_{i=1}^{q_j}, \tag{1}$$

without summation in $j$, where $N_j(x)$ is the PU function from the FEM.

The local approximation functions for the node $x_j$ are composed by $q_j$ linearly independent functions.

$$I_j \overset{def}{=} \{L_{j1}(x), L_{j2}(x), ..., L_{jq_j}(x)\} = \{L_{ji}(x)\}_{i=1}^{q_j}, \tag{2}$$

with $L_{j1}(x) = 1$.

The approximation $\tilde{u}(x)$ for the displacements field is given by eq. (3).

$$\tilde{u}(x) = \sum_{j=1}^{N} N_j(x) \left\{ u_j + \sum_{i=2}^{q_j} L_{ji}(x) b_{ji} \right\}, \tag{3}$$

where $u_j$ e $b_{ji}$ are nodal parameters associated with the components $N_j(x)$ e $N_j(x)L_{ji}(x)$, respectively.

### 2.1 Stable Generalized Finite Element Method

The SGFEM consists in a local modification on the GFEM enrichment. This modified enrichment is given by Babuška and Banerjee [3]:

$$\tilde{L}_{ji} = L_{ji} - I_{wj}(L_{ji}), \tag{4}$$

where $I_{wj}$ is the interpolation function defined by:

$$I_{wj}(L_{ji}) = \sum_{k=1}^{n} N_k(x) L_{ji}(x_k), \tag{5}$$

where $n$ refers to the number of nodal points of the element that contains the position $x$, $x_k$ is the vector of the coordinates of the node $k$ of the element that contains the position $x$ and $L_{ji}(x_k)$ is the original enrichment function of the GFEM, eq. (2).

The shape functions of the SGFEM are given by:

$$\{\phi_{ji}\}_{i=1}^{q_j} = N_j(x)\{\tilde{L}_{ji}(x)\}_{i=1}^{q_j}, \tag{6}$$

without summation in $j$.

In this paper, the ill-conditioning of the stiffness matrix is measured by the Scaled Condition Number ($C(\hat{K})$), according to Gupta et al. [6]. The scaled stiffness matrix $\hat{K}$ is given by:

$$\hat{\mathbf{K}} = \mathbf{DKD}, \tag{7}$$

where $K$ is the stiffness matrix and $\mathbf{D}$ is a diagonal matrix such that $D_{ij} = \frac{\delta_{ij}}{\sqrt{K_{ij}}}$.

In the software INSANE, the Scaled Condition Number $C(\hat{\mathbf{K}})$ is calculated by means of Singular Value Decomposition (SVD):

$$C(\hat{\mathbf{K}}) := \|\hat{\mathbf{K}}\|_2 \|\hat{\mathbf{K}}^{-1}\|_2 \tag{8}$$

### 2.2 Polynomial enrichment strategy

The polynomial enrichment strategy improves the approximate space in parts of mesh. In the work Duarte et al. [2], the autors suggested a transformation of the enrichment $L_{ji}(x)$ when the functions are polynomial. The coordinate $x$ is replaced by:

$$x \rightarrow \frac{x - x_j}{h_j}, \tag{9}$$

where $h_j$ is the diameter of the largest finite element that contains the node $j$.

The shape functions associated with a generic node $x_j$ for differents polynomial enrichment functions are given:

Linear Enrichment (P1): Equivalent to the approximation produced by a quadrilateral element Q8.

$$\phi_j^T(x) = N_j(x) \begin{bmatrix} 1 & 0 & \beta & 0 & \delta & 0 \\ 0 & 1 & 0 & \beta & 0 & \delta \end{bmatrix}, \tag{10}$$

Quadratic Enrichment (P2): Equivalent to the approximation produced by a quadrilateral element Q12.

$$\phi_j^T(x) = N_j(x) \begin{bmatrix} 1 & 0 & \beta & 0 & \delta & 0 & \beta^2 & 0 & \delta^2 & 0 \\ 0 & 1 & 0 & \beta & 0 & \delta & 0 & \beta^2 & 0 & \delta^2 \end{bmatrix}, \tag{11}$$

where $\beta = \frac{x-x_j}{h_j}$ and $\delta = \frac{y-y_j}{h_j}$.

### 2.3 Numerical enrichment strategy

The numerical enrichment strategy use the global-local strategy. This strategy is based in two scales, a global with a coarse mesh, and a local with a fine mesh. The process of enrichment is divided in three stages:

- First, the global problem is solved.

- The solution of the global problem is transferred as boundary conditions for the local problem. Then the local problem is solved.

- Lastly, the enriched global problem is solved where the solution of the local problem is used as enrichment function.

The application of this strategy for the solution of nonlinear analysis is based on a methodology presented in Monteiro et al. [7], named NL-GFEM$^{GL}$. In this methodology the nonlinear analysis is performed only in the global problem and in the end of each converged incremental step a local problem is solved. Each problem uses its own mesh, with the respective integration points, for the numerical integration.

Similarly to GFEM$^{GL}$, presented in [4, 8], the process is divided in three stages:

- The first stage is the solution of the first global incremental step. This step uses the global mesh without any enriched node.

- The second stage is the solution of the local problem. The local model is obtained from the global model in the region with damage. The data of the position, size and refinement level of this model are informed by the user. The boundary conditions of this problem are the solution of the global converged incremental step. Beyond the boundary conditions, the constitutive variables are also transferred to the local problem. These constitutive variables represent the state of material and are obtained through of the mapping process presented in Monteiro et al. [7]. The local problem is solved using a secant approximation to the stiffness matrix.

- The last stage is the solution of the enriched global problem for the next incremental step. The enrichment functions are the solution of the local problem and they are the same for all Newton-Raphson iterations. This enrichment functions can be modified by the stable strategy (eq. (4)). Once this global incremental step converges, a new local problem is solved for the new state of material.

The Fig.1 summarizes the process NL-GFEM$^{GL}$.

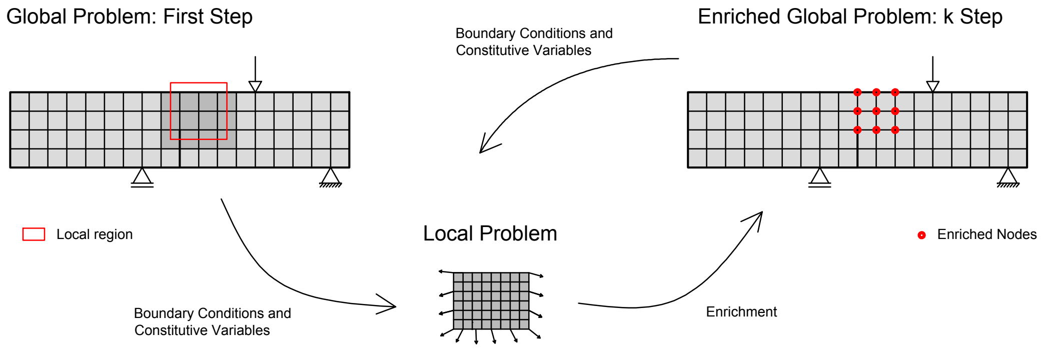


Figure 1. NL-GFEM$^{GL}$ process.

## 3 Numerical Simulations

In this section, a numerical experiment is presented to compare the different enrichment strategies applied to methods GFEM and SGFEM. This example refers to mixed mode fracture of concrete beams published by Gálvez et al. [9], Fig. 2, where three sizes of beams and two types of restraints (values of K) were tested. Herein, the model uses a medium size of beam and the type 1 of test that have $K = 0$. Figure 2 shows the geometry, loading and boundary conditions. The force $P$ is $1000N$. The constitutive model considered is the smeared cracking, presented in Gori et al. [10]. For this model, Carreira-Ingraffea laws are adopted. The material parameters adopted in the numerical simulation are the same to the experimentally measured ones: Young's modulus $E = 38000N/mm^2$, Poisson's ratio $\nu = 0.2$, fracture energy $G_f = 0.069N/mm$ and tensile limit stress $f_t = 3.0N/mm^2$. Besides these parameters other four parameters are necessary for application of the laws: compression limit stress $f_c = 54.0N/mm^2$, strain (relative to $f_c$) $\varepsilon_c = 0.0025$ and characteristic lenght $h = 25mm$.

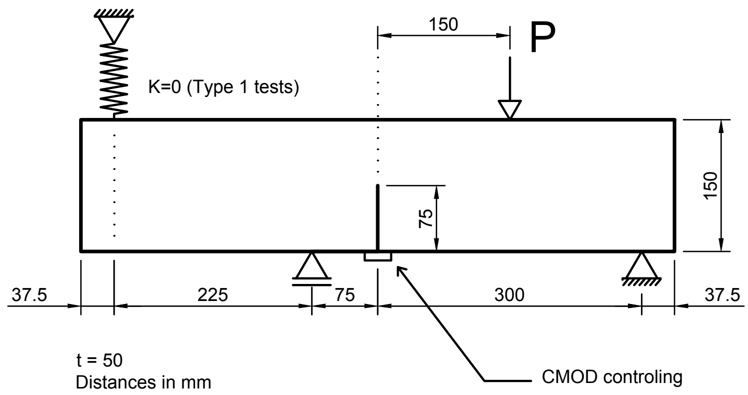


Figure 2. Geometry, loading and boundary conditions.

A coarse mesh with 288 elements is used to model this example. The elements are four-noded quadrilateral with 4x4 integration points. A total of 18 nodes are enriched in the region of the beam where the damage is propagated. A refinement of 2 times is used to generate the local elements. The local solution is used in the numerical enrichment strategy. Figure 3 shows the coarse mesh, the enriched nodes and the local refinement for the numerical enrichment.

The generalized displacement control is adopted for controlling the load incremental. The initial value of 0.1 is applied to load factor. The tolerance for convergence is $1\text{x}10^{-4}$ in relation to the norm of the vector of incremental displacements.

Figure 4 shows the experimental scatter and the numerical prediction of the load P versus Crack Mouth Opening Displacement (CMOD), as in Fig. 2, for the enrichment strategies and the coarse mesh (global mesh of the Fig. 3) with FEM. The enrichment strategies are: linear polynomial enrichment with GFEM (NL-GFEM-P1), quadratic polynomial enrichment with GFEM (NL-GFEM-P2), global-local enrichment with GFEM (NL-GFEM$^{GL}$) and global-local enrichment with SGFEM (NL-SGFEM$^{GL}$).

It is possible to observe that the coarse mesh is not able to represent the experimental results. The strategies with polynomial enrichment present a limit load and softening branch closest of the experimental one.

The global-local enrichment strategy with GFEM had similar behavior to the one observed for FEM coarse mesh. NL-GFEM$^{GL}$ presented, however, a superior limit load. On the other hand, with the application of the stable strategy, the numerical model was able to represent de experimental results.

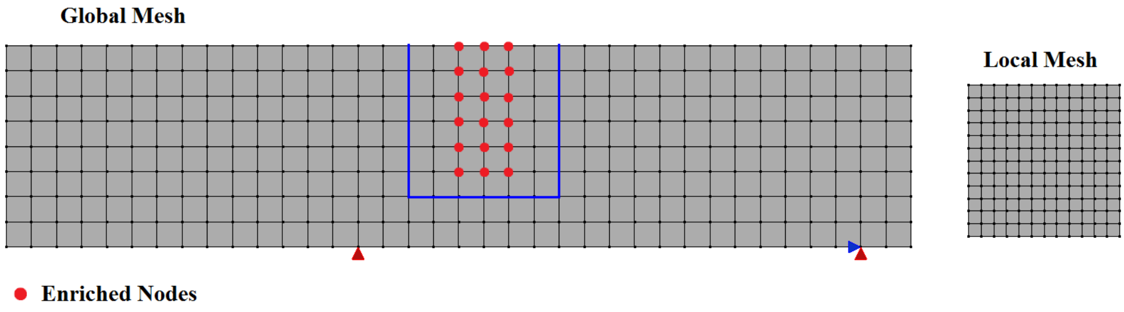


Figure 3. Coarse mesh, enriched nodes and local mesh.

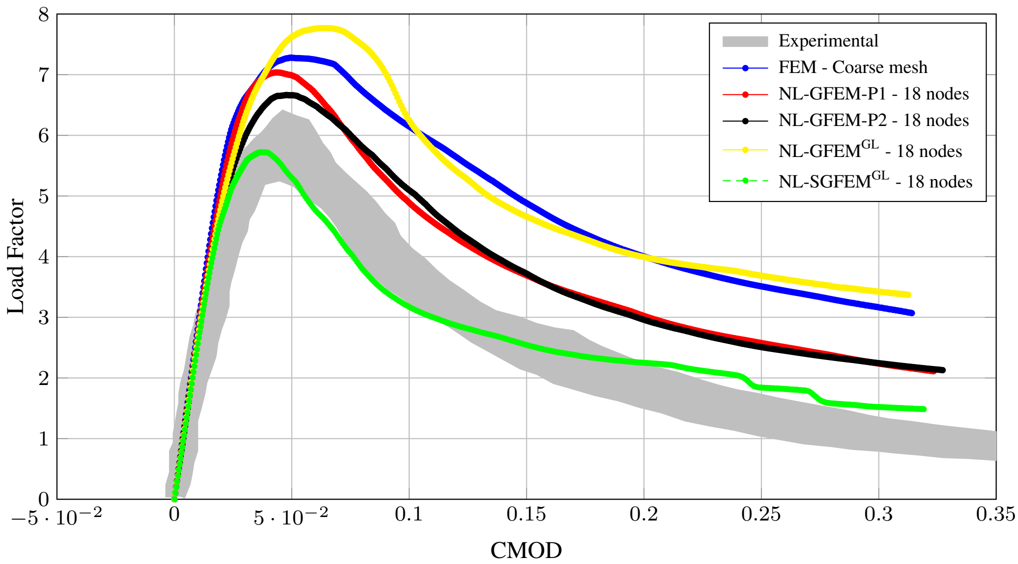


Figure 4. Equilibrium paths.

Figure 5 shows the logarithm of the condition number versus the step for the differents strategies. The condition number increase smoothly during the analysis for all strategies except for NL-GFEM$^{GL}$ strategy that shows a higher value for the condition number and decrease sharply. This instability problem is in accordance with the bad results presented for this strategy.

Figure 6 shows the evolution of the damage for the NL-SGFEM$^{GL}$ strategy in steps 50 (load factor = 4.509), 100 (load factor = 5.370), 200 (load factor = 2.872) and 500 (load factor = 1.484). Figure 7 shows the experimental envelope of the crack obtained by Gálvez et al. [9]. Its possible to observe that the evolution of the damage present a good approximation regarding the experimental scatter band.

Table 1 indicates the total number of iterations of the analysis and the number of degrees of freedom (DOFs) associated with enrichment strategies. This table shows that the NL-SGFEM$^{GL}$ is able to provide a more stable and more accurate result, with a smaller number of DOFs and iterations than the other strategies evaluated here.

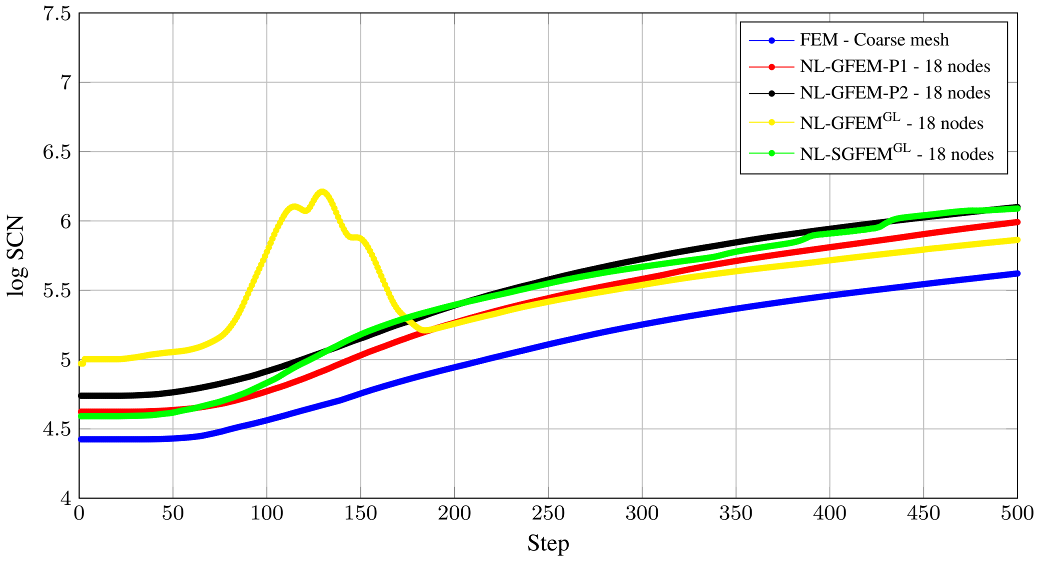


Figure 5. Scaled Condition Number (SCN) versus step.

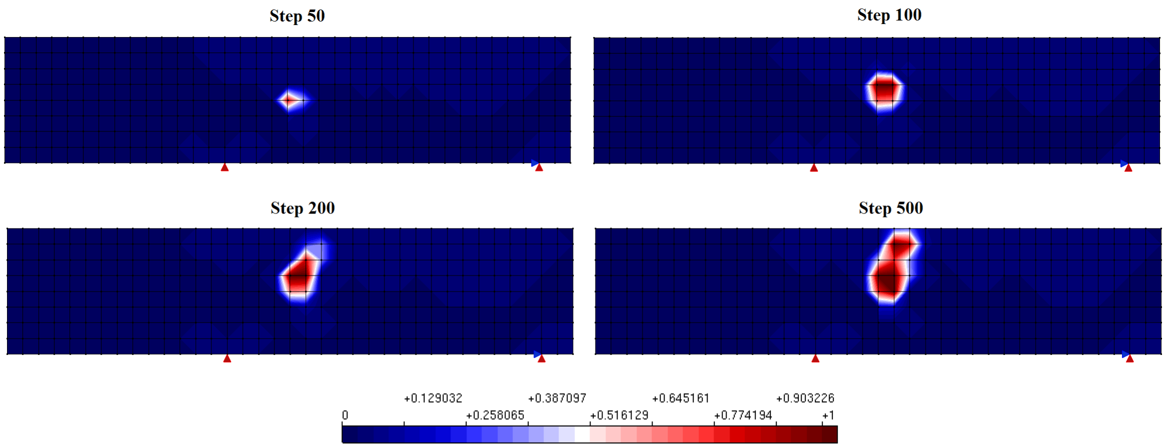


Figure 6. Evolution of the damage for NL-SGFEM$^{GL}$ strategy.

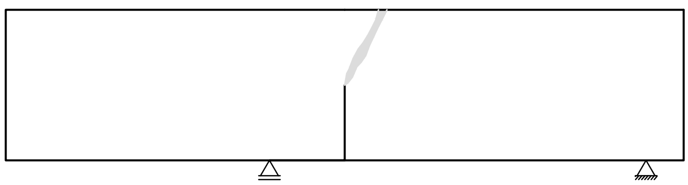

Figure 7. Experimental envelope of crack.

Table 1. Number of DOFs and total number of iterations.

| | DOFs | Iterations |
|---|---|---|
| FEM - Coarse Mesh | 674 | 2057 |
| NL-GFEM-P1 | 746 | 2163 |
| NL-GFEM-P2 | 818 | 2512 |
| NL-GFEM$^{GL}$ | 710 | 2289 |
| NL-SGFEM$^{GL}$ | 710 | 1711 |

## 4 Conclusions

This paper presented a comparison of different enrichment strategies applied to GFEM and SGFEM. Linear and quadratic polynomial enrichment and global-local enrichment were used in the simulations. An example of the mixed mode fracture with experimental results was used to compare the results. The same number of enriched nodes was used in all simulations.

The application of the polynomial enrichment presented better results if compared with the coarse mesh without enrichment. The quadratic enrichment shows a limit load lower than the linear enrichment but with a larger number of DOFs.

The global-local enrichment with GFEM was not able to reproduce the experimental results and presented some instabilities. On other hand, the application of the stable strategy was able to recover an accurate simulation of the experimental behavior. This strategy presented advantages when compared to polynomial enrichment, a smaller number of DOFs and of iterations.

The analisys of the condition number shows instabilities of the NL-GFEM$^{\mathrm{GL}}$ strategy. This fact can explain the bad results obtained by this approach for the equilibrium path.

**Acknowledgements.** The authors gratefully acknowledge the importante support of the Brazilian agencies FAPEMIG (in Portuguese “Fundação de Amparo à Pesquisa de Minas Gerais” - Grant PPM-00747-18), CNPq (in Portuguese “Conselho Nacional de Desenvolvimento Científico e Tecnológico” - Grants 309515/2017-3, 437639/2018-5 and 304211/2019-2) and CAPES (in Portuguese “Coordenação de Aperfeiçoamento de Pessoal de Nível Superior”).

**Authorship statement.** The authors hereby confirm that they are the sole liable persons responsible for the authorship of this work, and that all material that has been herein included as part of the present paper is either the property (and authorship) of the authors, or has the permission of the owners to be included here.

## References

[1] Strouboulis, T., Babuška, I., & Copps, K., 2000. The design and analysis of the Generalized Finite Element Method. *Computer Methods in Applied Mechanics and Engineering*, vol. 181, n. 1-3, pp. 43–69.

[2] Duarte, C. A., Babuška, I., & Oden, J. T., 2000. Generalized Finite Element Methods for three-dimensional structural mechanics problems. *Computer & Structures*, vol. 77, n. 2, pp. 215–232.

[3] Babuška, I. & Banerjee, U., 2012. Stable Generalized Finite Element Method (SGFEM). *Computer Methods in Applied Mechanics and Engineering*, vol. 201-204, pp. 91–111.

[4] Duarte, C. A. & Kim, D. J., 2008. Analysis and applications of the generalized finite element method with global-local enrichment functions. *Computers Methods in Applied Mechanics and Engineering*, vol. 197(6-8), pp. 487–504.

[5] Fonseca, F. T. & Pitangueira, R. L. S., 2007. An object oriented class organization for dynamic geometrically nonlinear. In *Proceedings of the CMNE (Congress on Numerical Methods in Engineering)/ CILAMCE (Iberian-Latin-American Congress on Computational Methods in Engineering)*.

[6] Gupta, V., Duarte, C., Babuška, I., & Banerjee, U., 2013. A stable and optimally convergent generalized FEM (SGFEM) for linear elastic fracture mechanics. *Computer Methods in Applied Mechanics and Engineering*, vol. 266, pp. 23–39.

[7] Monteiro, H. A. S., Novelli, L., Fonseca, G. M., Pitangueira, R. L. S., & Barros, F. B., 2020. A new approach for physically nonlinear analysis of continuum damage mechanics problems using the generalized/extended finite element method with global-local enrichment. *Engineering Analysis with Boundary Elements*, vol. 113, pp. 277–295.

[8] Evangelista, F., Alves, G. S., Moreira, J. F. A., & de Paiva, G. O. F., 2020. A global-local strategy with the generalized finite element framework for continuum damage models. *Computers Methods in Applied Mechanics and Engineering*, vol. 363.

[9] Gálvez, J. C., Elices, M., Guinea, G. V., & Planas, J., 1998. Mixed mode fracture of concrete under proportinal and nonproportional loading. *International Journal of Fracture*, vol. 94, pp. 267–284.

[10] Gori, L., Penna, S. S., & Pitangueira, R. L. S., 2017. A computational framework for constitutive modelling. *Computers and Structures*, vol. 187, pp. 1–23.